

Alignment of the DELPHI vertex detector

V. Chabaud, A. Andreazza, P. Collins, H. Dijkstra

Abstract

This note describes the procedures used to align the DELPHI vertex detector. It also gives an account of unexpected problems met in the 1994 alignment, in particular the one resulting from LEP beams acollinearity. Results are given on the precision achieved in the alignment.

1 Introduction

This note gives a fairly detailed account of the procedures which have been developed to align the DELPHI Microvertex detector (VD), versions 1992-1993 and 1994-1995.

VD92-93 had 3 layers, all measuring only $R\phi$ coordinates (Ref. [1]).¹ VD94-95 has also 3 layers but the innermost and outermost ones now measure both $R\phi$ and z coordinates (Fig. 1 and Ref. [2]). The innermost layer has been lengthened in view of the forward-backward extension planned for next year, so that only the outermost and intermediate layers will be rebuilt for VD96. Aside from the obvious benefit for physics, we have found that the availability of z coordinates has made the process of aligning the VD significantly easier and safer, especially as regards the relative alignment of the two half-shells. In order to keep the size of this note within reasonable limits, we shall restrict ourselves to the alignment of VD94-95, but should point out that a large fraction of the procedures used for $R\phi$ alignment have been borrowed from the alignment of VD92-93.

Before going to the details, it is worth mentioning two things:

- the pioneering work of R. McNulty, responsible for the alignment of VD90 and VD91 (Ref. [3]);
- the importance of the interaction which has taken place between the aligners and the designers of the “next” version of VD, through the lessons learned during the alignment of the current version VD (VD96 will be the 4th version of the Delphi Microvertex detector!).

Section 2 will give a short description of the VD. Section 3 will give a résumé of the optical and mechanical survey operations. In Section 4 we shall describe in detail the alignment procedures, with some emphasis on detector specific effects like “Lorentz drift” and “barycentric shift” as well as on twist effects. Section 5 will dwell on 3 unexpected complications which were met for the 1994 alignment. To conclude, results on the precision achieved in the VD alignment will be given in Section 6.

2 Short description of the VD

VD94-95 consists of 3 layers that we call Closer, Inner and Outer respectively. Each layer consists of 24 overlapping modules (about 10% overlap in $R\phi$ for Closer and Outer modules and 20% for Inner modules). Each module consists of 4 detectors, two “central” and two “extreme” ones (Fig. 1). A half-module consists of one central and one extreme detector bonded in series and read-out at either end.

Double sided readout has been introduced for Closer and Outer layers, enabling them to measure z coordinates as well as $R\phi$ ones. An original solution has been chosen for the assembly of the two detectors forming a half module of Closer or Outer layers. Traditionally they are joined by daisy-chaining p-side readout lines to p-side ones and n-side to n-side. Here the n-side lines of one detector are joined to the p-side ones of the other detector (Fig. 2). This so-called “flipped module” design has the advantage that the noises on the two sides of a detector are equalized, thereby improving the S/N performance of the n-side signals from both detectors. Another advantage is that the signal polarity tags which detector of a half-module produced a signal. A third advantage, benefiting the

¹We shall use the standard DELPHI coordinate system where the x axis is horizontal pointing toward the LEP centre, the y axis is vertical and the z axis is horizontal along the electron beam. ϕ is the azimuthal angle in the xy plane and θ is the polar angle with respect to the z axis.

quality of the alignment will be explained in Sect. 4.3.

For all 3 layers even-numbered modules are shifted by 5 mm along z with respect to the odd-numbered ones (Fig. 1). Aside from the normal overlaps in $R\phi$ of a central (extreme) detector with the adjacent central (extreme) ones, we therefore have also some small areas where a central detector overlaps in $R\phi$ and in z the adjacent extreme ones, or where a central detector on the $z > 0$ side overlaps the adjacent ones on the $z < 0$ side. We shall see in Sect. 4.3 the usefulness of these “double overlap” regions for a refinement of the z alignment.

Practically, in order to make feasible the installation of the VD inside DELPHI, it has been constructed as 2 independent half-shells, consisting of 12 full sectors each and overlapping each other at top and bottom after insertion. For either half-shell, the outer ends of each module are mounted on 2 aluminum semi-circular structures which surround the beam pipe. The mechanical structure is water cooled and the water temperature is kept constant during data taking to ensure a good mechanical stability of the VD (a temperature change of 1°C makes the VD expand by 5 μm along a diameter). Two methods are used to monitor the position of the VD after insertion inside DELPHI. The first one uses a series of laser light spots mounted on the inner wall of the surrounding Inner Detector and shining on the VD Outer layer. The second one is based on the reconstruction of tracks from Z^0 decays passing through the overlap regions between adjacent modules. The first method, no longer available from 1995 onward, monitors the position of the VD with respect to the Inner Detector, while the observation of tracks in overlap regions (for all 3 layers) provides a purely internal check of the mechanical stability of the VD, especially of the relative position of the 2 half-shells.

3 Survey of the VD

The survey of the VD involves 2 stages. After assembly, all the modules are individually measured optically to define the strips position with respect to two reference spheres. Afterwards, when the modules are mounted on the end rings, a full three dimensional survey of the complete half shells is performed before the insertion in DELPHI (Ref. [4]).

3.1 3D measurement of individual modules

A camera² mounted on the same 3D measurement station³ employed for the global survey and having a $250\times$ magnification provides a precision of 2 μm on the focal plane and 15 μm in the coordinate orthogonal to the focal plane. Each module has two high precision machined 4 mm diameter reference spheres positioned on the readout hybrids. The positions of the strips on both sides of each of the 4 detectors are measured with respect to the strips of the others, as well as with respect to the reference spheres.

3.2 3D survey of full half-shells

The 3D measurement station uses a mechanical probe. One measures, for each half-shell separately, the relative position of all reference spheres, as well as the “planes” of all

²Mondo Machine Developments Ltd., Leicester UK.

³POLI S.p.A, Varallo Sesia, Italy.

individual detectors on one side of each module. Each half-shell is measured in 2 steps. First, Inner and Outer half-layers are assembled and the 3D measurement is performed on these 2 layers. Next, Closer half-layer is mounted and is surveyed together with Outer layer, again. For either step each half-layer is measured 2 or 3 times. The precision of the mechanical survey is $3 \mu m$ for the spheres position and $23 \mu m$ for the detector plane radial position.

When the survey of a half-shell is completed, the 2 series of measurements are superimposed via the common Outer half-layer and the 3D modules measurements are merged with the resulting overall 3D survey. At this stage a global survey precision of $25 \mu m$ in the strip position is obtained. Finally, after insertion of the VD inside DELPHI, one performs a rough alignment of the half-shells with respect to the other detectors, using muon pair tracks from Z^0 decays, which provides the initial data base that will be the starting point of the refined alignment described in the next Section.

4 Alignment of the VD

4.1 General

Here follow a number of “guidelines” which have been found extremely important for an optimum alignment.

- The software alignment should deal with the task of aligning $3 \times 24 = 72$ full modules (432 degrees of freedom) and not 4 times more constituent detectors. Full modules must be measured with enough precision by the Mondo and Poli machines and remain stable during the several months of data taking. Even more than the difficulty of tackling $4 \times 432 = 1728$ degrees of freedom the problem would be the practical impossibility to collect rapidly enough tracks (especially muon pairs) to achieve a sufficient alignment precision for the detectors at large (or small) θ . This question of sufficient statistics will become crucial at LEP200.

- For safety and efficiency one should strive first to align the VD purely internally, then to align the resulting rigid body externally with respect to the rest of DELPHI. Reasons are twofold. At least two detectors (Inner Detector and TPC) require a lengthy calibration at the start-up of each year and they even rely on the VD to perform part of their calibration. Also projecting the possible distortion of another tracking detector into the (no longer purely) internal alignment of the VD might become terribly difficult to disentangle.

- Tracks passing in the overlap region of adjacent modules are an essential ingredient of alignment. They are also very useful for monitoring the stability with time of the VD.

- Even if a MINUIT-like program were available to determine the 432 parameters of the internal VD alignment, within a tolerable execution time, the results would be miserable. There are always remaining local (or even global) distortions of the actual VD with respect to its ideal geometrical description which would fool the MINUIT-like program. We need a sequential and iterative program allowing us to monitor the quality of the alignment at every step, to diagnose problems related to some specific parameters and, if necessary, to introduce adhoc “massage” of these parameters. After various attempts we have been led to the following procedure, fulfilling these requirements. Outer layer is assigned the status of *master* layer, while Closer and Inner layers are treated as *slave*

ones. By that we mean that Outer layer is aligned as a *full* pseudo-cylindrical object using all $R\phi$ and z overlap constraints between adjacent modules. Closer and Inner layer modules are then aligned *individually* with respect to the corresponding Outer modules. One could certainly imagine other, equivalent, alignment procedures. In particular one would be forced to do so if, unluckily, one full module of Outer layer would die after installation, thereby breaking its geometrical continuity.

- Given the lightness of the mechanical structure of the VD, some overall distortion (called “twist” for short) of the shape of either half-shell might be induced during the insertion of the VD inside DELPHI. Special care should be taken to diagnose and correct these effects. Actually we have found that some parameters like the z position of individual modules might have been altered by up to 10 times the precision of the survey!

Our procedure uses 3 types of tracks from Z^0 decays: hadronic tracks passing through the overlap region of 2 adjacent sectors (we call them “overlap tracks”), hadronic tracks within one sector (“3-hit tracks”) and muon pair tracks passing within 2 opposite sectors (“ $\mu\mu$ tracks”). The $\mu\mu$ tracks are assigned momenta equal to the precisely known beam energy of LEP, so that the only information borrowed from the other tracking detectors is the momentum of overlap tracks and of 3-hit tracks.

Three types of residuals (in $R\phi$ or in z) are defined from these tracks. For overlap tracks, if we want to study Outer layer alignment in $R\phi$, we constrain an arc of circle to pass through a hit in Closer or in Inner layer and one of the 2 hits in Outer layer. We call “ $R\phi$ overlap residual” in Outer layer the residual formed from the second hit. To form z overlap residuals one has to use an arc of helix and to substitute $R\phi + z$ hit doublets for $R\phi$ hits. For 3-hit tracks we constrain an arc of circle to pass through the Closer and Outer layer hits and call “3-hit residual” the residual formed from the Inner layer hit. For $\mu\mu$ tracks we constrain an arc of circle (or helix) to pass through the 2 $R\phi$ hits (or hit doublets) in opposite sectors of Outer layer and call “ $R\phi$ (or z) $\mu\mu$ residuals” the residuals formed from the $R\phi$ hit (or hit doublet) in either of the 2 corresponding opposite sectors of Closer layer (Fig. 3).

4.2 Initial alignment

After installation the VD position with respect to the other detectors is known with a few mm precision. Using loose criteria for the association of hits to external tracks, the first $\mu\mu$ tracks collected at LEP are used to refine this positioning to better than 100 μm .

Another trivial but time-consuming task is the chase for possible cabling errors in the VD readout electronics as well as for gross errors in the initial database, which might come from an incorrect assembling of the Mondo $R\phi$ or z measurements of the constituent 4 detectors of some modules.

4.3 Special effects: Lorentz drift and barycentric shift

The magnetic field in DELPHI causes the holes and electrons to drift at a small angle relative to the electric field in the detectors. This effect is harmless for the z coordinates but must be cured for the $R\phi$ ones. Due to the flipped module design the resulting shift of the reconstructed hit is in an opposite direction in the central and extreme detectors of the Outer or Closer modules. This Lorentz drift can be studied using 3-hit tracks. Fig. 4 shows the mean $R\phi$ 3-hit residual as a function of the z coordinate of the track in the

Outer layer. Two jumps appear at the transition between central and extreme detectors of Outer layer modules, corresponding to a Lorentz drift of $6 \mu\text{m}$. This value is consistent with that obtained using a previous method [1], and is applied to both the Closer and Outer layers.

During this study it was also found that the barycentres of the holes and of the electrons do not correspond exactly to the mid-plane of detectors. For the holes in the Outer (Closer) layer this new effect can be seen when studying the $R\phi$ residuals in Outer (Closer) layer of overlap tracks. Fig. 5 shows the mean $R\phi$ overlap residual in the Outer layer as a function of the z coordinate of the track in the same layer. The two jumps correspond again to the transition between central and extreme detectors. Using the relative inclination of the two plaquettes (15°) we deduce a barycentric shift of $10.5 \mu\text{m}$.

The barycentric shift of the electrons cannot be measured in a similar way since its effect on z overlap residuals is cancelled out for tracks passing through the overlaps of central detectors as well as of extreme detectors. But it can be measured when comparing the z overlap residuals of tracks passing through the small “double overlap” regions to the z residuals of “normal” overlap tracks.

Using these procedures barycentric shifts of holes and electrons in Closer and Outer layers have been found to range between 10 and $20\mu\text{m}$, all toward the p-side of detectors.

Note that Lorentz drifts are invisible with overlap tracks since the E-field direction is the same in adjacent detectors. Conversely, the effect of $R\phi$ barycentric shift is suppressed in 3-hit tracks since the majority of the tracks pass through a region where the detector planes are parallel, and hence a radial displacement induces no $R\phi$ shift. We do not have yet a physical explanation for the barycentric shift effect and do not know of a confirmation from other experiments. But to observe it with an arrangement of “non-flipped” detectors one would have to survey the relative position of the various detectors with a micron precision, if not the barycentric shift would be “swallowed” by the alignment with tracks and become invisible!

The Lorentz drift in $R\phi$ as well as the $R\phi$ and z barycentric shifts are corrected for in the initial database before proceeding to the Microvertex detector alignment.

4.4 Internal alignment

4.4.1 Frames of reference and geometrical variables

The 24 sectors are numbered circularly in order of increasing ϕ starting from top. One half-shell consists of sectors 1-12, the other one of sectors 13-24. For the needs of the internal alignment, 2 cartesian frames are chosen, one for each half-shell. Following the DELPHI naming, we call B half-shell the one consisting of sectors 1-12 and D half-shell the one consisting of sectors 13-24. Fig. 6 depicts the 6 geometrical variables (3 translations SLID, DELRAD, SLIZ and 3 rotations ROTA, DIPZ, WIGZ) involved in the alignment of each module. The frame of reference of the B half-shell is chosen as the base reference for the overall internal alignment and 6 more geometrical variables are introduced to represent the 3 translations (called TRXD, TRYD, TRZD) and the 3 rotations (called ETAXD, ETAYD, ETAZD) needed in the alignment of the D half-shell with respect to the B half-shell.

4.4.2 Internal $R\phi$ and z alignment of Closer and Outer layers

This is the most complex operation in the VD alignment. It uses overlap tracks and $\mu\mu$ tracks. As already mentioned we assign Outer and Closer layers the status of *master* and *slave* layers, respectively. By that we mean that *all* $R\phi$ and z overlap constraints between adjacent modules of Outer layer will be used to fully align (reconstruct) that layer. Closer layer modules will then be individually aligned with respect to the corresponding Outer modules. Overlap residuals of Closer layer are not used in the alignment but serve only as a crosscheck of the alignment quality.

Outer modules 6 and 18 play a privileged role; they can be considered as “hinges” of the 2 half-layers.⁴ Some reflection shows that the parameters SLID(6), SLID(18), DELRAD(6), DELRAD(18), SLIZ(6), SLIZ(18) have to be kept frozen during the alignment; indeed one must all the same align objects with respect to something! As we shall see ROTA(6) and ROTA(18) play also a very special role.

The relative alignment of the 2 half-shells is achieved via the $R\phi$ and z overlap constraints of Outer layer. The $R\phi$ overlap residuals at top (sectors 24/1) and bottom (sectors 12/13) allow us to determine TRXD, ETAZD, ETAYD and $\delta = \text{ROTA}(18) - \text{ROTA}(6)$.⁵ The quantity δ is the *relative* twist of the 2 half-shells which might have been induced during insertion of the VD inside DELPHI. Practically we alter ROTA(18) by the amount δ and we shall see later how to cure a possible overall twist which is now carried by ROTA(6).

In a similar fashion the z overlap residuals at top and bottom allow us to determine TRZD, TRYD and ETAXD.⁶

As already said the alignment of either half-shell of Outer layer is achieved via the $R\phi$ and z overlap constraints. The $R\phi$ overlap residuals allow the determination of $\text{SLID}_{Out}(i)$ and $\text{ROTA}_{Out}(i)$, $i \neq 6, 18$. The z overlap residuals allow the determination of $\text{SLIZ}_{Out}(i)$ and $\text{DELRAD}_{Out}(i)$, $i \neq 6, 18$.

The alignment of the individual modules of Closer layer is achieved using $\mu\mu$ tracks. The $R\phi$ $\mu\mu$ residuals allow the determination of $\text{SLID}_{Clo}(i)$ and $\text{ROTA}_{Clo}(i)$, $i = 1$ to 24. The z $\mu\mu$ residuals allow the determination of $\text{SLIZ}_{Clo}(i)$ and $\text{DELRAD}_{Clo}(i)$, $i = 1$ to 24. Note that the $R\phi$ $\mu\mu$ residuals could also be used to determine $\text{DELRAD}_{Clo}(i)$, but they give less precision than the z residuals and serve only as a further crosscheck of the alignment quality.

4.4.3 Internal $R\phi$ alignment of Inner layer

This is a much simpler operation. Once Closer and Outer layers are internally aligned, individual modules of Inner layer are aligned with respect to the corresponding Closer and Outer modules, using constraints from 3-hit tracks. This operation provides SLID_{Inn} ,

⁴Since a half-shell contains an even number of sectors, one might as well have chosen modules 7 and 19 instead of 6 and 18.

⁵The overlap residuals distributions are fitted with the function: $r = r_0 + k * Z$, Z being the average z of each overlap track in the Outer layer; the sum of the r_0 's at top and bottom gives TRXD and their difference gives ETAZD; the sum of the k 's at top and bottom gives ETAYD and their difference gives $\delta = \text{ROTA}(18) - \text{ROTA}(6)$.

⁶The overlap residuals distributions are fitted with the function: $r = r_0 + k * \cot \theta + h * \cot^2 \theta$; the difference of the r_0 's at top and bottom gives TRZ, the sum of the k 's gives TRYD, the sum of the h 's gives ETAXD; note that a non-zero value of the sum of the r_0 's or of the difference of the k 's or of the difference of the h 's would indicate a deviation of the shape of the VD from our geometrical model.

ROTA_{Inn} and DELRAD_{Inn} for all 24 modules of Inner layer. Overlap tracks are not used in this operation and the $R\phi$ overlap residuals between adjacent Inner modules are used as a cross-check of the quality of the overall alignment.

4.4.4 Implementation and limitations of the internal alignment program

For brevity let us only say that the 2 stages of the alignment procedure (Outer+Closer, then Inner) are sequential and iterative at many levels and that the various steps⁷ are sequenced so that convergence is reached as efficiently as possible, which is especially important for the first stage.

Input data for the 3 types of tracks is prepared in the form of compact mini DSTs on disk files to permit repeated execution of the program in a reasonable amount of time when studying the effects of some critical and reluctant alignment parameter(s).

Care was taken in the fits to the various residuals to discard outlier hits from background or misassociation in an unbiased and robust way. Repeated regressions are performed on the sample of residuals. At each iteration an estimate of the standard deviation is made and residuals larger than about 2.5σ are excluded from the new regression. Four to five iterations give a satisfactory fit.

At LEP 1 there is no limitation to the number of available overlap and 3-hit tracks. As for $\mu\mu$ tracks 100 tracks/sector is the very minimum for a sensible alignment. Life becomes comfortable with 300 tracks/sector (which is equivalent to about 150,000 hadronic Z^0 decays taking into account the actual efficiency of the VD). With two to three times as many overlap and 3-hit tracks per sector one run of the internal alignment program takes 5 to 10 mins on an HP720.

The reader has noticed that our procedure does not have access to all geometrical variables of Fig. 6. Indeed the parameters WIGZ and DIPZ are difficult to measure and they are set to zero. One might observe that DELRAD and WIGZ are complementary parameters and that our procedure charges DELRAD for deviations which might actually come from the other one. Strictly speaking this is incorrect. This pragmatic choice is justified by the smallness of the values found for DELRAD as well as by the overall quality of the alignment.

4.5 Overall twist suppression and twist in general

The best method used to measure and remove any overall twist is based on the study of the geometrically signed impact parameter of 3-hit tracks with respect to the beam spot as a function of their polar angle θ . Any dependence on θ reveals a twist (see the Appendix for a demonstration of the principle of this method). To remove overall twist one has to make one or two iterations between the “twist program” and the internal alignment one.

One could also use cosmic tracks. Unlike $\mu\mu$ tracks they do not all pass close to the centre of the VD and, for those approaching the z axis at large positive or negative z , the effect of twist on their geometry is much amplified. Any dependence of their $R\phi$ residuals on z reveals a twist (the definition of residuals of cosmic tracks is the same as for $\mu\mu$ residuals, see Sect. 4.1).

The two methods agree well in measuring the value of ROTA_{Out}(6) needed to suppress overall twist. A typical twist of either half-shell with respect to the Poli measurements

⁷Seven basic steps to align Outer+Closer layers, two to align Inner layer.

might correspond to shifts of the Outer layer $R\phi$ strips of say $150 \mu m$ at $z = 100$ mm.

It is time now to go deeper into the understanding of twist. All we have said previously has been oversimplified. What happens during the insertion of the VD inside DELPHI? Let us press toward each other or pull apart 2 diagonally opposite corners of a half-shell.⁸ Three sorts of distortions appear:

- The 2 edges along z of the half-shell are no longer parallel. This effect is well represented by our parameter ROTA(6) (or ROTA(18)).

- A shear deformation along the z direction developed throughout the 12 modules. This effect could be represented by a uniform variation of the parameters SLIZ(1) to SLIZ(12).

- The 12 modules, assumed to be flat before pressing, are now individually twisted about their z axes (a bit more intuition is required to perceive this effect). This deformation should be visible in the distribution of the z overlap residuals.

In addition this exercise predicts a unique sign correlation between the 3 effects.

All these effects were already found at the overall 3D survey stage and they are fully confirmed by the results of the VD94 alignment. Half-shell D happened to be badly twisted, B much less. After alignment we found that all Outer modules of half-shell D had been assigned a large, quasi constant ROTA correction and a SLIZ correction varying almost linearly with the module number (Fig. 7). The twist of individual modules can be seen via the z overlap residuals and we found indeed a general U-shape of these residuals as a function of z (Fig. 8). All 3 effects have the expected sign correlation and a further confirmation came from the alignment of VD95 for which it turned out that half-shell B and not D was more severely twisted.

The observation of twist for individual modules implies relaxing partly the first “guideline” stated in Sect. 4.1. The shape of individual modules *must* be and *can* be obtained from the 3D survey of the VD but it has to be corrected to represent individual twists. This effect has little influence on the precision of tracks in the $R\phi$ view but must absolutely be corrected for the Rz one. Practically a database is generated by the alignment program as if there were no module twists but a radial correction is applied to each hit reconstructed within the database from its local coordinates x_l and z_l inside the corresponding module. The radial correction is parametrized as $\delta R = k * x_l * z_l$. The constant k is assumed to be the same for all modules of a given layer and a given half-shell. For VD94 δR was reaching $35 \mu m$ at the corners of the Outer modules of half-shell D.

4.6 External alignment

Finally the rigid body obtained from the previous steps is aligned externally. The alignment constants (three translations and three rotations) are determined using muon pair tracks reconstructed in the other tracking detectors of DELPHI and minimizing the sum of their squared residuals inside the VD with the MINUIT program.

At this stage we have found that our procedure for internal alignment might induce a small coherent distortion of the geometrical shape of the VD. All internal $R\phi$ or z residuals distributions look satisfactory but when reconstructing $\mu\mu$ tracks through the VD hits and extrapolating them into the Outer Detector (OD) for instance, one finds that

⁸It is more practical and less dangerous to construct a model from a thin PVC drain pipe that we cut loose into 2 half-cylinders and to play with one of them.

the mean $R\phi$ residuals with respect to the OD hits show a periodic dependence on ϕ of the form $A * \cos(2\phi - \phi_0)$, where the amplitude A might be as large as $150\mu m$.

Observing strongly different phases ϕ_0 for the alignments needed for the 4 quasi-stable periods of 1994 (see Sect. 5.2) and for 1995 convinced us that this effect was an artefact of the alignment procedure. An explanation might be the non-rigorous treatment of the variables DELRAD and WIGZ (see Sect. 4.4.4). This distortion is cured by a variant of the internal alignment program where the SLID parameters of the Outer modules are altered by an amount $a * \cos(2\phi - \phi_0)$ (with $a \simeq 0.05 * A$) and the alignment of individual modules of Closer and Inner layers is repeated. This “massage” looks well justified if one notices that the resulting imposed offsets of the $R\phi$ overlap residuals in the “master” Outer layer seldom exceed $1\mu m$.

5 Unexpected complications for VD94 alignment

Three problems were found during the alignment of VD94:

- a rather large radial bending of Closer and Outer modules with respect to the shape measured during the survey;
- an equally large mechanical instability of the VD throughout the data taking period;
- a significant time dependent acollinearity of the LEP beams during the same period.

5.1 Radial bending of Closer and Outer modules

This effect was first observed through a puzzling and very large S-shaped dependence of the mean $\mu\mu$ miss distance in the Rz view as a function of θ (amplitude up to $300\mu m$). It was further observed as a general U-shape of the $R\phi$ overlap residuals of Outer and Closer modules as a function of z , with amplitudes of about 12 and $25\mu m$ respectively, corresponding to a radial bending about 4 times larger (Fig. 9).

A long investigation revealed two causes for the radial bending.

1) Closer layer modules are stiffened by gluing a $270\mu m$ Ω -shaped kevlar beam along each module. Outer layer modules are stiffened by gluing ceramic rails $3.5mm$ wide, $0.6mm$ thick along the two edges of each module. The rigidity of these stiffeners was smaller than for VD92-93 modules but had been chosen to cope with the nominal pressure of the mechanical probe of the 3D measuring machine. For technical reasons it turned out that the actual pressure during the survey had been significantly larger than intended.

2) VD92-93 modules were stiffened with carbon fibre Ω -shaped beams. The upgrade to double-sided readout modules entailed the replacement of the conductive carbon fibre material by non-conductive kevlar one. It is well known that kevlar is hygroscopic but it had been somehow overlooked that a change of humidity might induce a change of the shape of individual modules.

To cure radial bending one must first measure it precisely. Using an alignment without correction and assuming that radial bending is the same for all modules of either layer, a polynomial in z is fitted to the $R\phi$ overlap residuals of all modules (excluding overlaps 24/1 and 12/13). The radial bending is given by multiplying this polynomial by a factor 4. Now the alignment is repeated in a way similar to the one used for twist correction of individual modules (see Sect. 4.5). The final database is generated by the alignment program as if

there were no radial bending but a radial correction must be applied independently to each hit reconstructed within the database. Fig. 10 shows the result of this procedure.

Several actions have been taken on the hardware front to minimize radial bending for VD95 and VD96. The pressure of the measuring probe has been checked and reduced as much as possible. The stiffening beams of Closer layer modules have been strengthened for VD95. A new design has been developed for VD96 which reduces significantly the coupling beam/detector when humidity varies. Finally humidity must be monitored and adjusted optimally in the survey lab.

5.2 Mechanical instability of the VD

After solving the problem of radial bending it was found that the VD had not been stable throughout the data taking period (May to November 1994). An indication of this effect had been given on-line by the laser light spots, but with much less precision than the overlap tracks. It looked as if the 2 half-shells had been steadily pivoting about their bottom support rails and moving away from each other at the top. This relative motion was irregular with a sequence: slow (during 2 months), fast (a few days), stable (3 months) and slow again (2 months). At the end of the year the displacement had reached about $120 \mu m$.

It is most likely that this misfortune was the consequence of problems met during the installation of the VD at the beginning of the year. After insertion the VD had to be removed, fixed-up and reinstalled in a hurry. One half-shell was not handled with enough care and internal stresses probably developed and were released with time leading to VD instability. This scenario looks all the more plausible that the almost identical VD95, whose installation went very smoothly, remained stable throughout the 5 months of data taking with LEP 1.

As regards the alignment of VD94, the practical solution has been to identify 4 quasi-stable periods and to make 4 independent alignments.

5.3 Acollinearity of LEP beams

After solving the second problem some serious inconsistencies were found between the relative alignments of the 4 tracking detectors (VD, ID, TPC and OD). This problem was eventually traced back to a significant and time dependent acollinearity of the electron and positron beams in the vertical plane (up to $0.25 mrad$). One can therefore no longer represent the trajectories of a muon pair by a single helix and practically one has to obtain from LEP the acollinearity parameters for each fill and introduce the appropriate kink between the trajectories of the 2 muons of each pair.

For convenience we give here the “kink formulae” valid for horizontal or vertical acollinearity as well as lack of momentum balance of the LEP beams.

Let us define:

\vec{p}_{e-} = momentum vector of LEP electron⁹

\vec{p}_{e+} = momentum vector of LEP positron

(as usual vector magnitude will be denoted by the same symbol without an arrow)

$$\vec{S} = \vec{p}_{e-} + \vec{p}_{e+}$$

⁹Warning: recall that electrons run along $+z$ and positrons along $-z$!

$\alpha_x = S_x/p_{LEP} =$ acollinearity angle in horizontal plane

$\alpha_y = S_y/p_{LEP} =$ acollinearity angle in vertical plane

where $p_{LEP} \simeq p_{e-} \simeq p_{e+}$

$\vec{p}_1 =$ momentum vector of first muon

$\vec{p}_2 =$ momentum vector of second muon

$\phi, \theta =$ azimuth and polar angle of momentum vector of first muon

$\vec{p}_{*1} =$ projection of vector \vec{p}_1 onto xy plane

$\vec{p}_{*2} =$ projection of vector \vec{p}_2 onto xy plane

The kink angle in the xy plane is given by the formula:

$$\alpha_* = -\alpha_x * \sin \phi / \sin \theta + \alpha_y * \cos \phi / \sin \theta$$

with the sign correspondence:

$\alpha_* > 0 \implies \vec{p}_{*1} \wedge \vec{p}_{*2}$ along $+z$

$\alpha_* < 0 \implies \vec{p}_{*1} \wedge \vec{p}_{*2}$ along $-z$

Let us further define:

$\tan \eta_1 = p_{1z}/p_{*1}$ (where dip angle $\eta_1 = \pi/2 - \theta_1$)

$\tan \eta_2 = p_{2z}/p_{*2}$ (and dip angle $\eta_2 = \pi/2 - \theta_2$)

$\epsilon = \eta_1 + \eta_2$

The difference ϵ of the absolute values of the dip angles is given by the formula:

$$\epsilon = -\cos \theta [\alpha_x * \cos \phi + \alpha_y * \sin \phi] + \sin \theta * S_z/p_{LEP}$$

with the sign correspondence:

$\epsilon > 0 \implies \vec{p}_1 \wedge \vec{p}_2$ parallel to $\vec{p}_{*1} \wedge \vec{z}$

$\epsilon < 0 \implies \vec{p}_1 \wedge \vec{p}_2$ antiparallel to $\vec{p}_{*1} \wedge \vec{z}$

6 Results

Before turning to an analysis of the quality of the alignment, let us notice that our results confirm the global survey precision of $25 \mu m$ quoted in Sect. 3. To see that one can look at the distributions of the variables DELRAD, ROTA or SLIZ and discard the superimposed smooth effect of the overall twist of either half-shell. Taking for instance Fig. 7 and fitting 2 low order polynomials through the ROTA distributions and similarly through the SLIZ ones, one finds remaining scatters compatible with $25 \mu m$.¹⁰

As regards the alignment, its quality is best judged when comparing *intrinsic* hit precision, measured from residuals which suffer little from misalignments, to *effective* hit precision obtained from residuals which include remaining misalignments. Upper limits for $R\phi$ intrinsic precision are measured from residuals of overlap tracks in Outer layer and residuals in Inner layer of 3-hit tracks tate (Fig. 11). After putting in the appropriate geometrical factor the $R\phi$ intrinsic hit precision is found to be better than $7.6 \mu m$. The effective hit precision is measured from residuals of overlap tracks in Closer or Inner layers, which have not been used as constraints in the alignment procedure (Fig. 11). One finds hit precisions of $8.8 \mu m$. The excess of this number over the above limit of $7.6 \mu m$ indicates the quality of the alignment. Another, complementary measurement of the effective hit precision is provided by the $R\phi$ miss distance between two muon tracks

¹⁰A variation of ROTA of $1 mrad$ corresponds to an $R\phi$ displacement of $115 \mu m$ at the end of a module.

(Fig. 12). From the observed $\sigma = 28\mu m$ one derives an impact parameter resolution of $20\mu m$ and an effective hit precision of $7.6\mu m$!. A third measurement (Ref. [2]) based on the study of the impact parameter of selected tracks with respect to the primary vertex gives results identical to the latter.

Similar results are obtained for z . An upper limit of the intrinsic z precision at $\theta = 90^\circ$ is measured from z residuals of overlap tracks in Outer layer (Fig. 13). Putting in the appropriate geometrical factor the z intrinsic precision is found to be better than $9.2\mu m$. The effective hit precision is provided by the z miss distance between two muon tracks (Fig. 12). From the observed $\sigma = 48\mu m$ at $\theta = 90^\circ$ one derives an effective precision of $12.5\mu m$.

The above discussion and the corresponding Figures indicate that it is difficult to quote a precise number to characterize the quality of the alignment. The various residuals distributions are not gaussian and display more or less pronounced tails; intrinsic hit precision is not the same for different layers and might even vary from module to module because some modules are significantly noisier than the others; we have found that the radial bending (Sect. 5.1) is not exactly the same for all modules of a given layer and we have cured it with a unique correction; finally we have also found that the relative alignment of the top and bottom modules of the two half-shells is slightly worse than the one of two modules of the same half-shell, which is not surprising considering the idea of aligning the 24 modules of Outer layer as 4 “flaps” secured to 2 “hinges” fairly remote from the top and bottom overlaps.

To give approximate numbers anyway, we estimate the alignment precision to be of the order of *half* the intrinsic precision (measured at $\theta = 90^\circ$ for z), namely better than or equal to $4\mu m$ in $R\phi$ and slightly larger than or equal to $5\mu m$ in z .

7 Appendix: Principle of the method for Overall twist suppression

Let us consider an ideal VD, perfectly aligned, and 4 particular muon pair tracks originating from a point-like beam spot at $X = Y = Z = 0$ and traversing Outer layer for instance at $Z = -10$ cm (points A^-, B^-, C^-, D^-) and at $Z = +10$ cm (points A^+, B^+, C^+, D^+) (see Fig. 14A). Staying in the reference frame of the database resulting from the survey, the effect of an overall twist induced at insertion time can be represented by a small rotation of the 4 points at $Z = -10$ cm and an opposite rotation of the 4 points at $Z = +10$ cm (Fig. 14B). The 4 muon pair tracks no longer pass through a common point. Now let us project Fig. 14B onto the $R\phi$ plane (Fig. 14C). The mean beam spot is still at $X = Y = 0$ but the 4 muon pair tracks have finite impact parameters with respect to it. The $R\phi$ alignment of the twisted VD will move the Closer layer modules so that the Closer hits of the muon pair tracks (lower case letters) be aligned with the corresponding Outer hits and one sees that the geometrically signed impact parameters of *single* muon tracks with respect to the mean beam spot have opposite signs for tracks at $Z = -10$ cm and tracks at $Z = +10$ cm. More generally the impact parameter of single tracks is proportional to Z (or to $\cot\theta$).

Practically the overall twist is measured and cured by studying the impact parameter, not of single muon tracks, but of the much more numerous 3-hit tracks from hadronic Z^0 decays.

References

- [1] The DELPHI Microvertex detector, N. Bingefors et al., Nucl. Instr. and Meth. **A328** (1993) 447.
- [2] The DELPHI Silicon Strip Microvertex Detector with Double Sided Readout, V. Chabaud et al., CERN-PPE/95-86, Nucl. Instr. and Meth. **A368** (1996) 314.
- [3] The Alignment of the DELPHI Microvertex Detector, R. McNulty, DELPHI 92-40 TRACK 69.
- [4] A. Andreazza et al., Nucl. Instr. and Meth. **A312** (1992) 431.

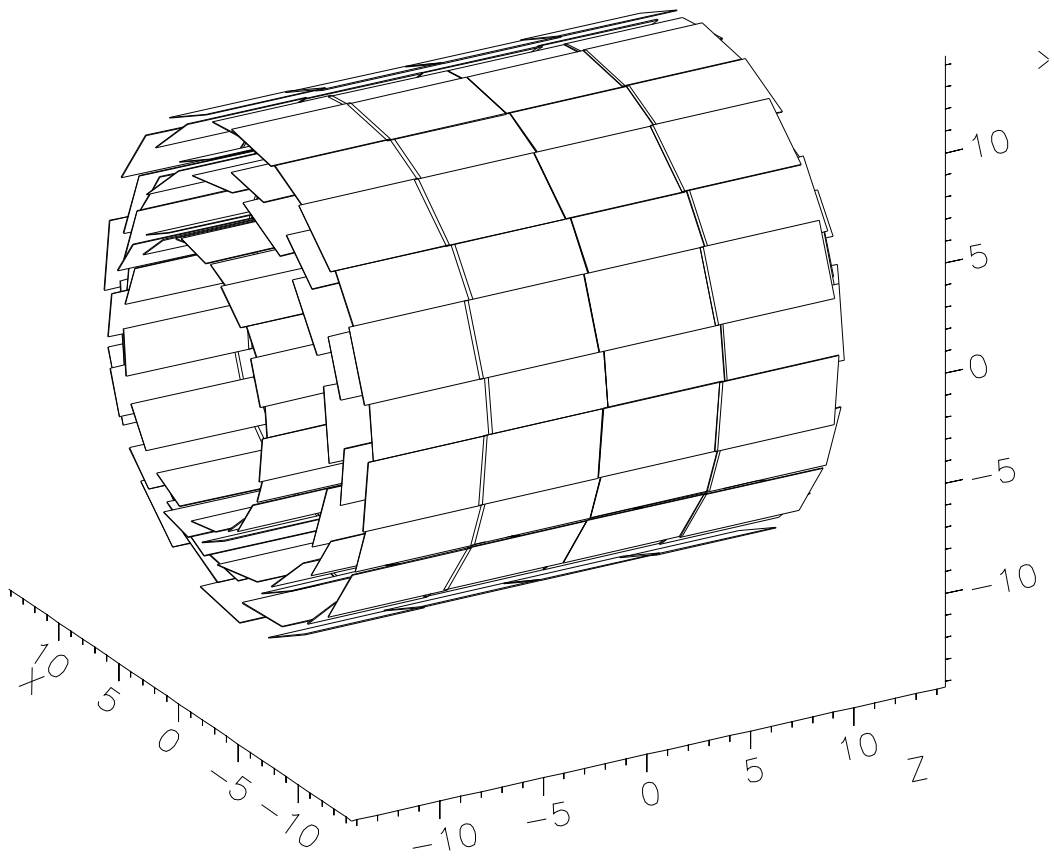


Figure 1: Perspective view of VD94-95. Closer layer was extended to cover polar angles between 25° and 155° . One also notices the larger overlap between adjacent modules of Inner layer, as well as the 5 mm staggering along z between odd- and even-numbered modules (more conspicuous for Outer layer).

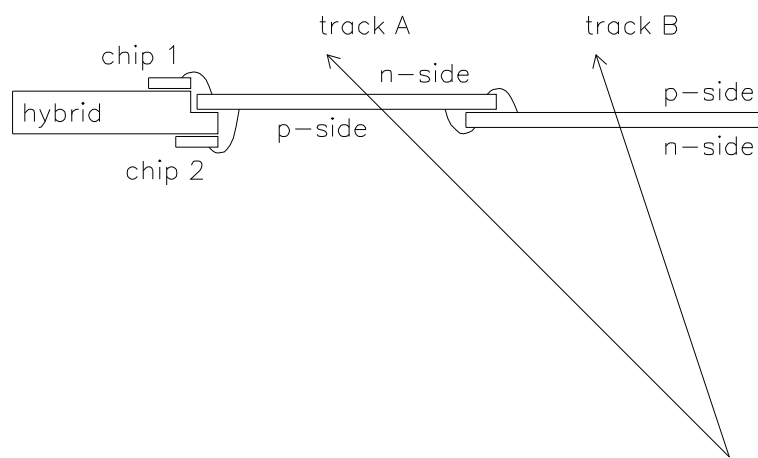


Figure 2: A schematic drawing of the flipped module concept. Chip 1 will register a negative (positive) signal from track A (B), while chip 2 will register a positive (negative) signal from track A (B). Positive signals correspond to $R\phi$ coordinates, while negative signals give the z -coordinate of tracks.

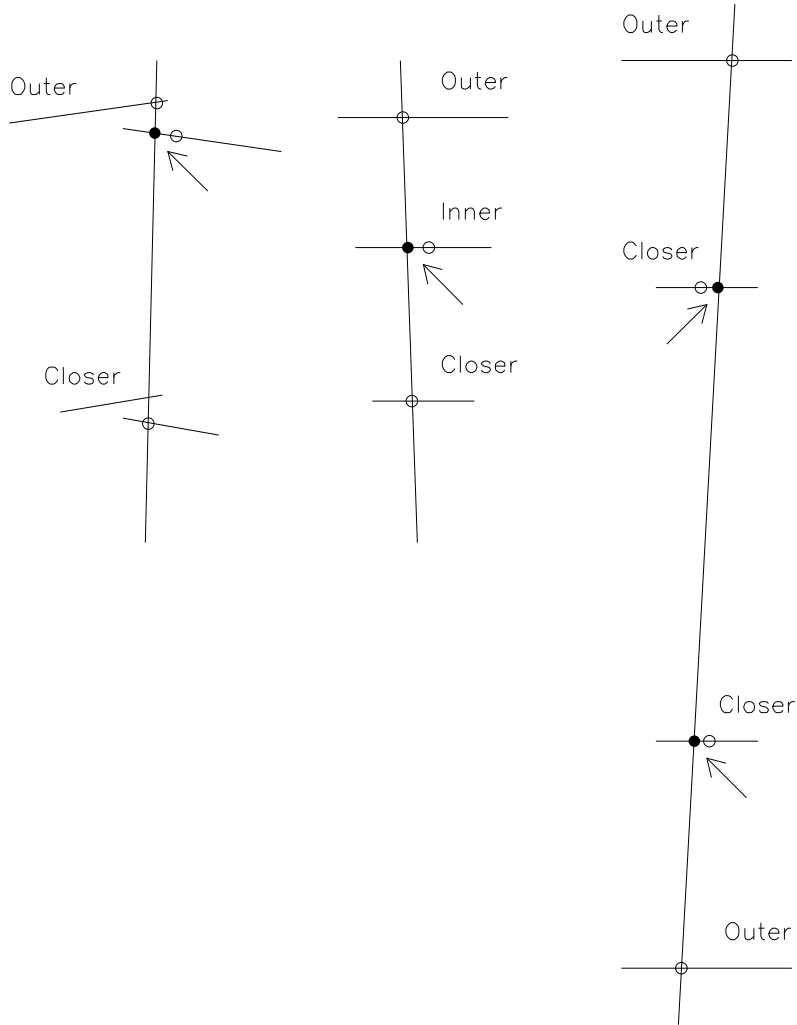


Figure 3: Schematic definition of $R\phi$ residuals for overlap tracks, 3-hit tracks and $\mu\mu$ tracks. Empty dots correspond to real hits, black dots to predicted hits from the other 2 real ones. The small curvature of tracks has not been represented. The definition of z residuals is similar, with residuals being measured along the z axis.

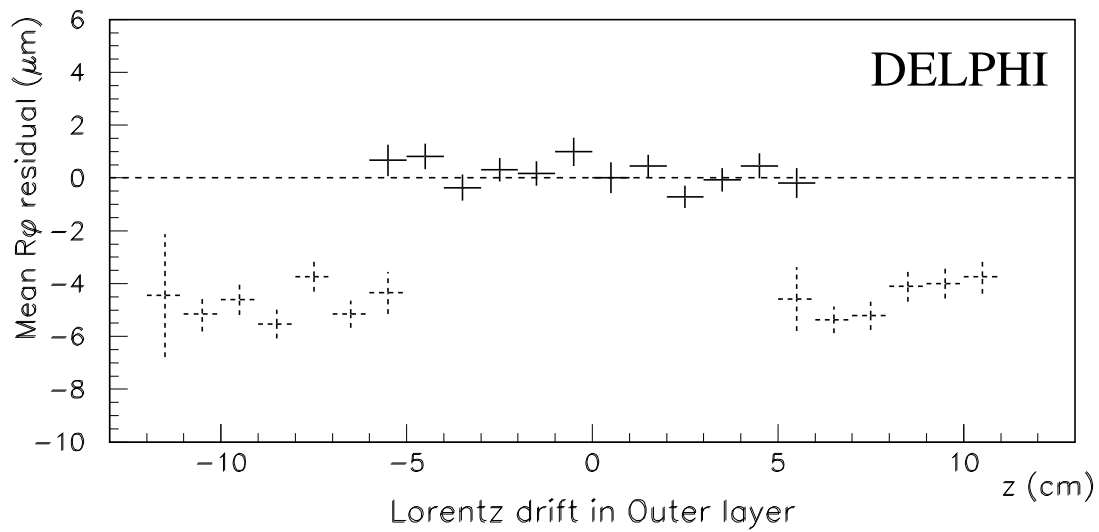


Figure 4: Mean residual in $R\phi$ for 3-hit tracks as a function of z at the Outer layer. Due to the flipped module design the E-field direction changes sign at around $|z| = 6\text{cm}$, while for both Inner and Closer layers the field remains in the same direction in the polar angle interval covered by the Outer layer.

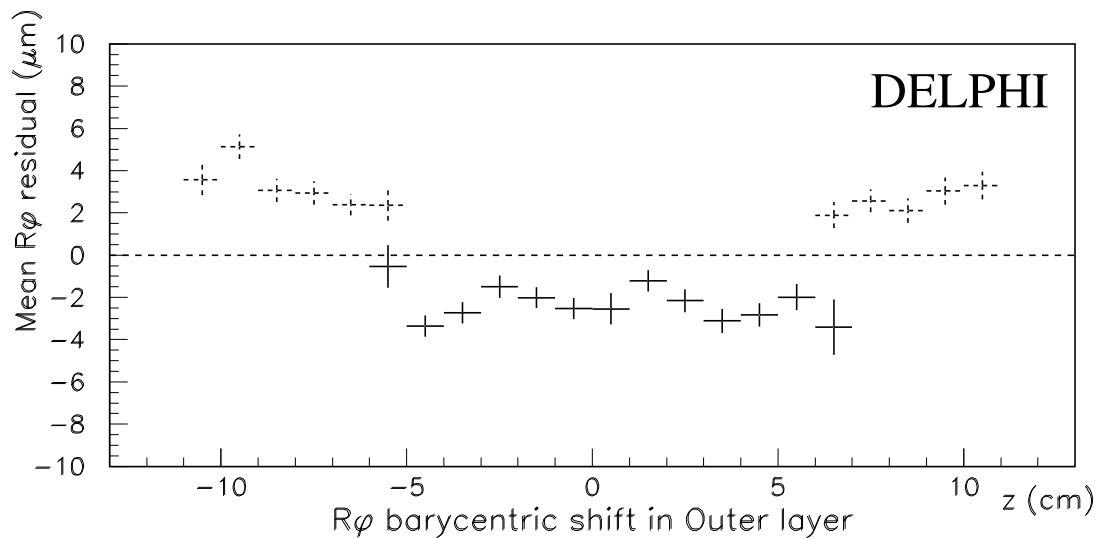


Figure 5: Mean residual in $R\phi$ for overlap tracks as a function of z at the Outer layer. Adjacent detectors have a relative angle of 15° . Hence a radial displacement δr will appear as a shift of close to $\delta r/4$ in the $R\phi$ residual. Due to the flipped module design a barycentric shift appears as a discontinuity at $|z| = 6\text{cm}$.

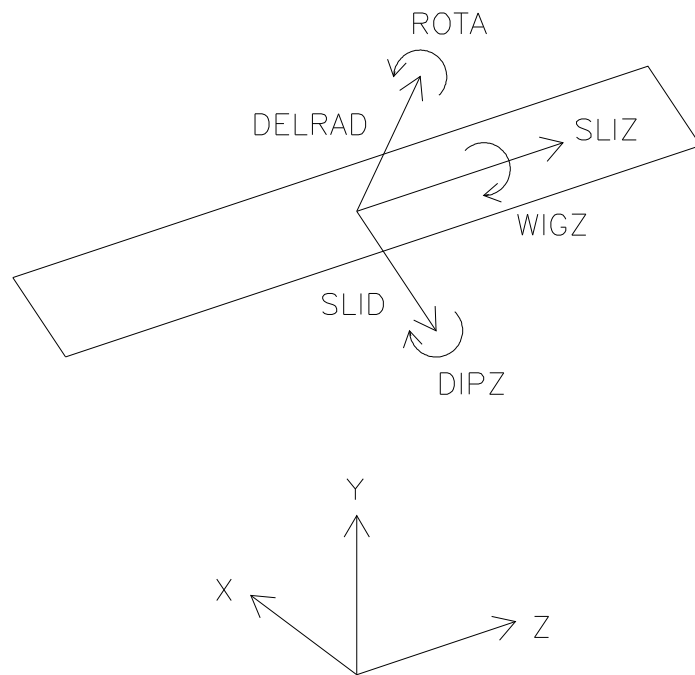


Figure 6: Sketch of the 6 geometrical variables involved in the alignment of individual modules.

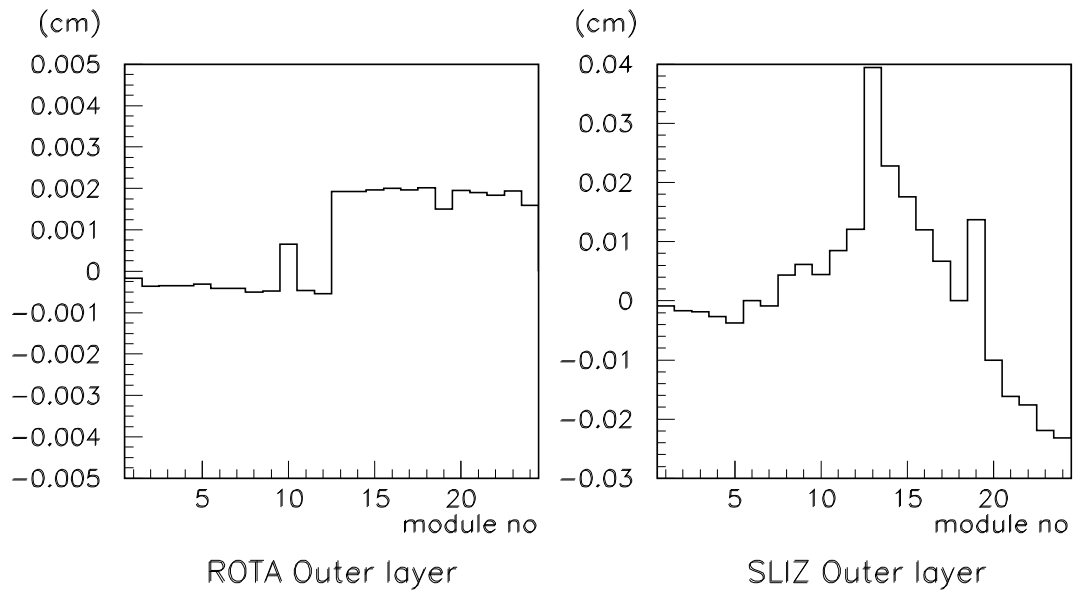


Figure 7: Distribution of the alignment variables ROTA and SLIZ as a function of the corresponding module number (1-12=half-shell B, 13-24=half-shell D) for VD94. The large twist of half-shell D is clearly demonstrated. The 3 spikes correspond to modules which had to be replaced or dismantled and remounted after the survey.

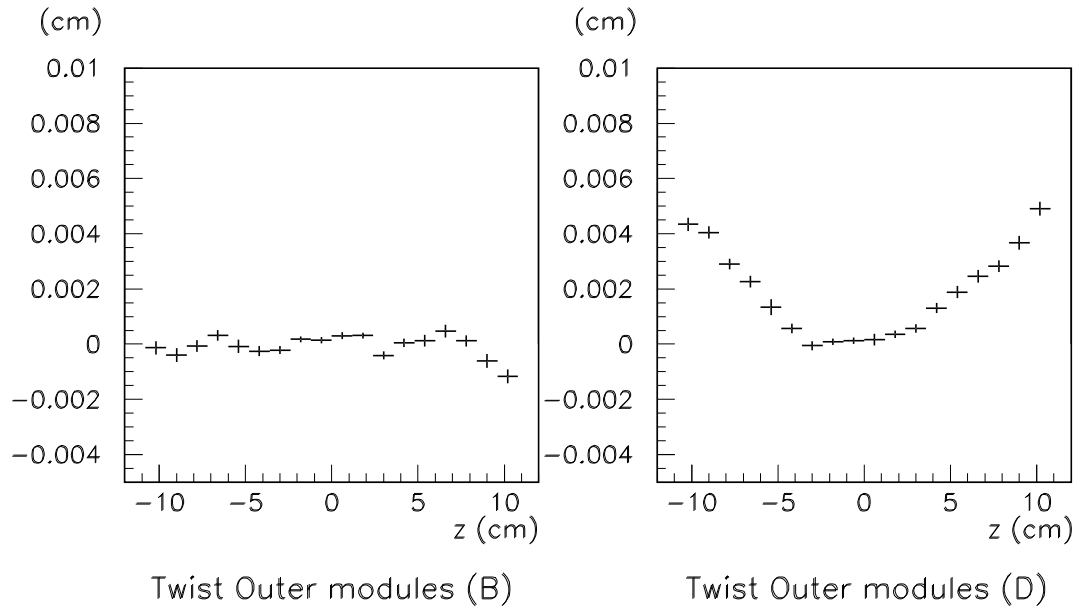


Figure 8: Distribution of the mean z residuals of overlap tracks in Outer layer as a function of z at the Outer layer for the 2 half-shells of VD94. The twist of the individual modules of half-shell D is clearly demonstrated.

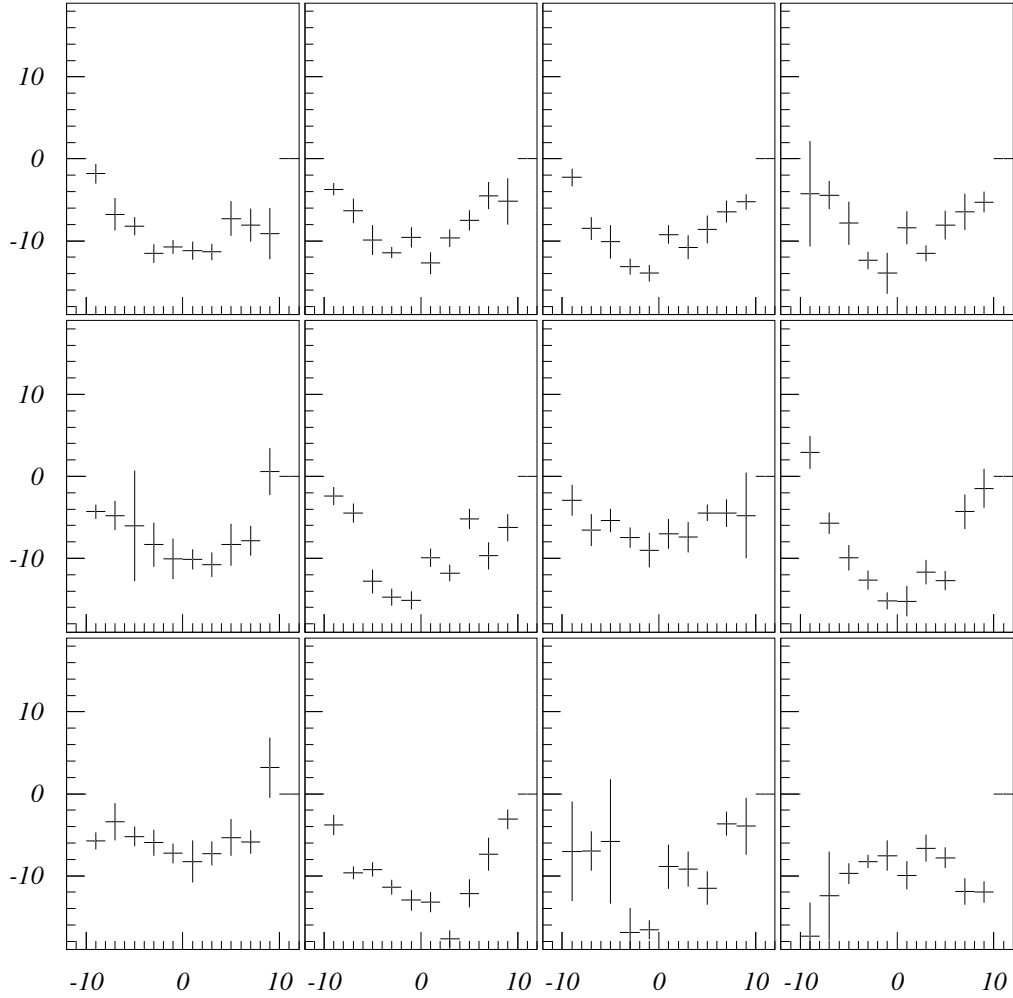


Figure 9: Distributions of the mean $R\phi$ residuals of overlap tracks in the first 12 modules of Outer layer as a function of z at the Outer layer for VD94. Units are μm and cm respectively. Radial bending is betrayed by the general U-shape of the distributions.

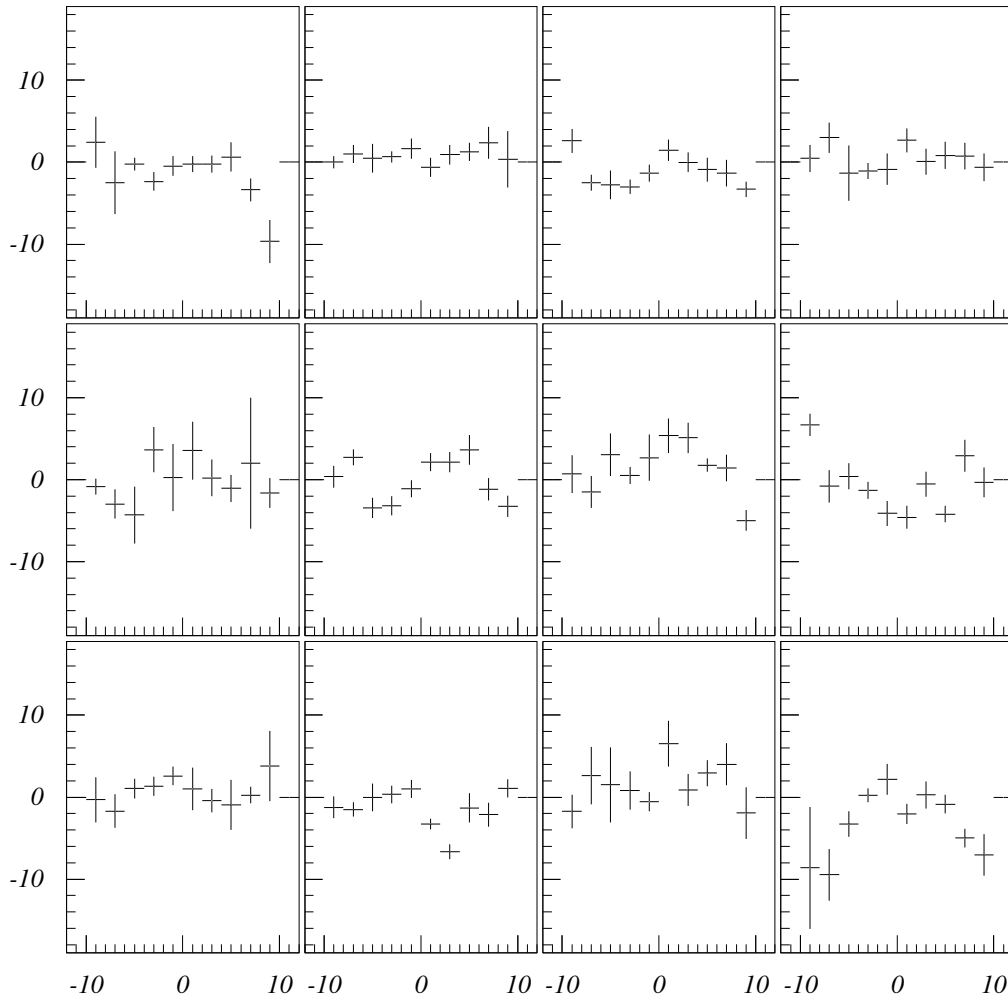


Figure 10: Distributions of the mean $R\phi$ residuals of overlap tracks in the first 12 modules of Outer layer as a function of z at the Outer layer for VD94, after radial bending correction. The distributions are generally flat except for one or two modules which should have bent a little more or a little less than the others.

DELPHI

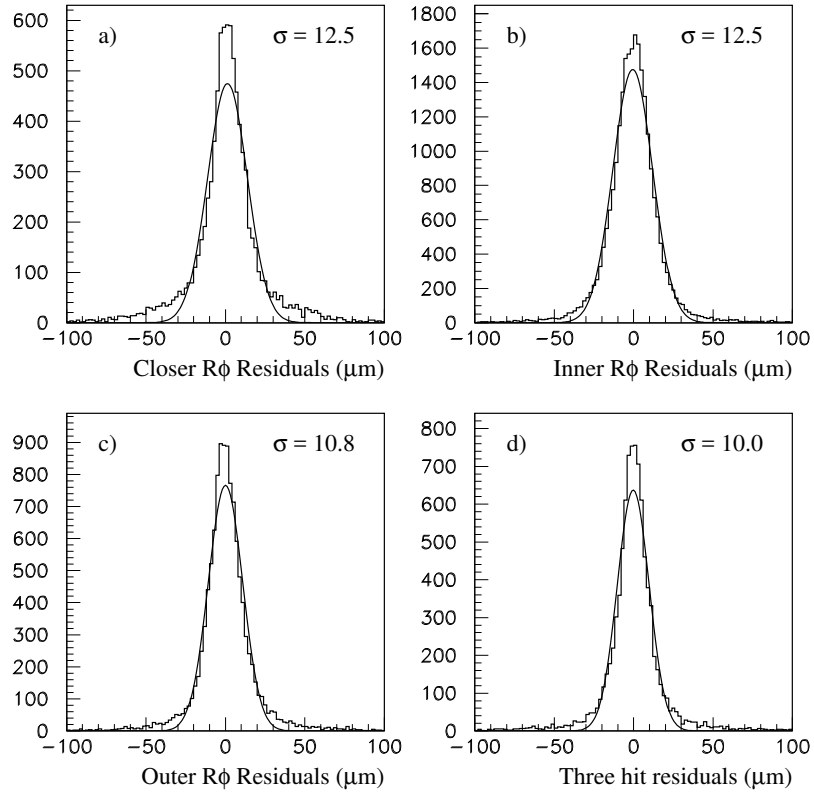


Figure 11: Residual distributions for a) Closer overlap tracks, b) Inner overlap tracks and c) Outer overlaps tracks. The width of each distribution has to be divided by $\sqrt{2}$ to exhibit the single hit precision for that layer of the vertex detector. Also shown are d) the Inner layer residuals for 3-hit tracks. Here the width has to be divided by $\sqrt{1.5}$ to obtain the silicon precision, assuming that it is the same in each of the three layers.

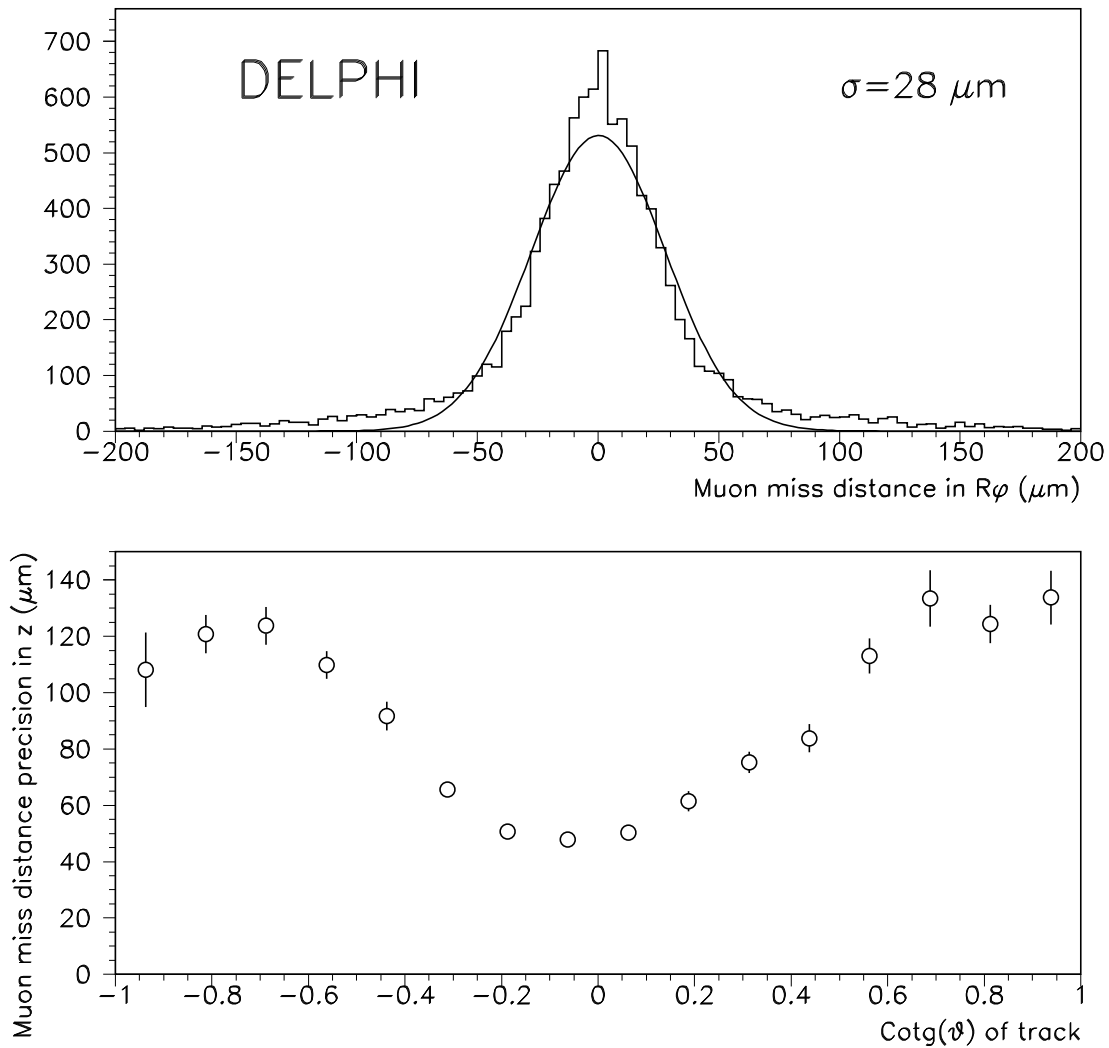


Figure 12: a) Miss distance between the two muons in $Z^0 \rightarrow \mu^+\mu^-$ in $R\phi$ plane; b) Miss distance between the two muons in $Z^0 \rightarrow \mu^+\mu^-$ in Rz plane as a function of the track polar angle.

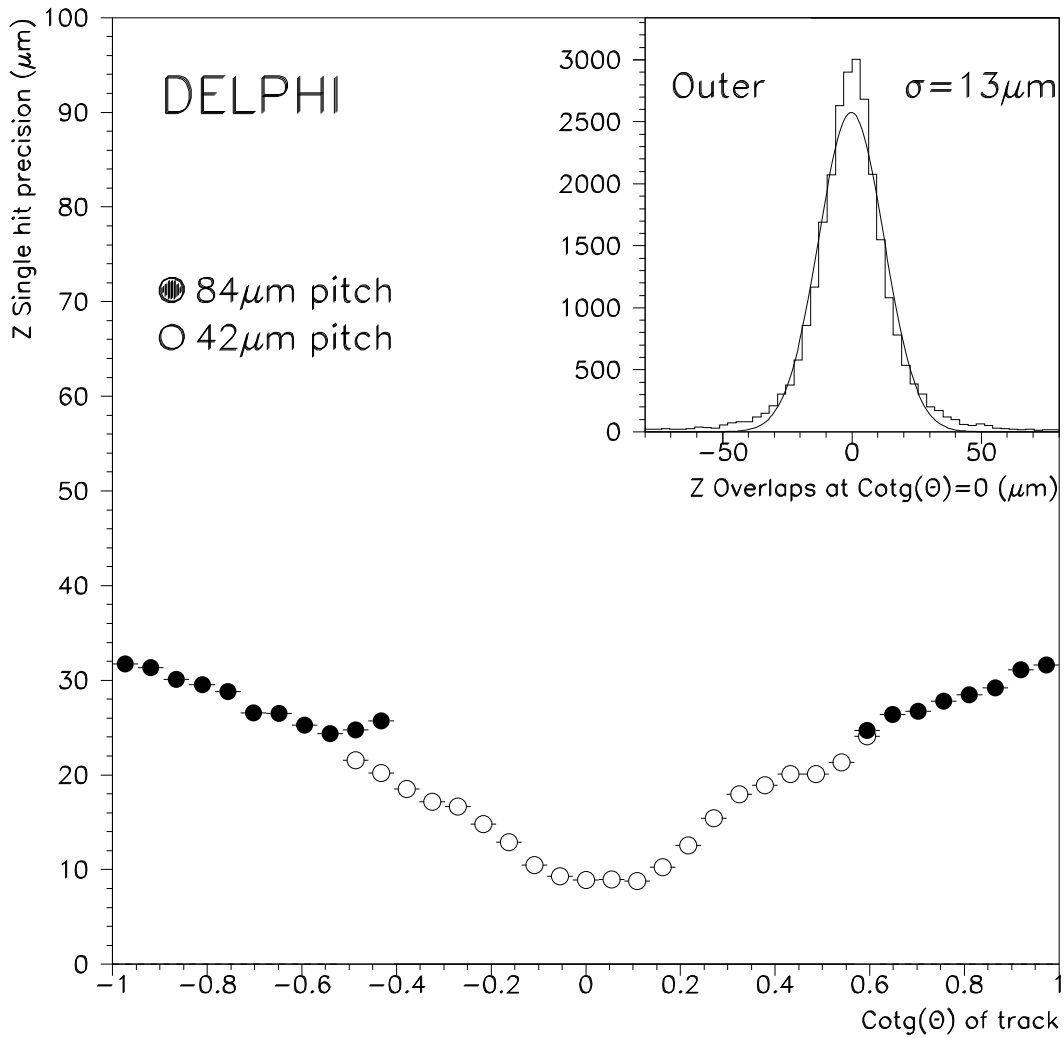


Figure 13: Outer layer z hit precision as a function of the track incident angle. The closed circles represent the region where the pitch was doubled. In the inset, z hit residuals for perpendicular particles. The width of the distribution has to be divided by $\sqrt{2}$ to obtain the single hit precision for that layer of the vertex detector.

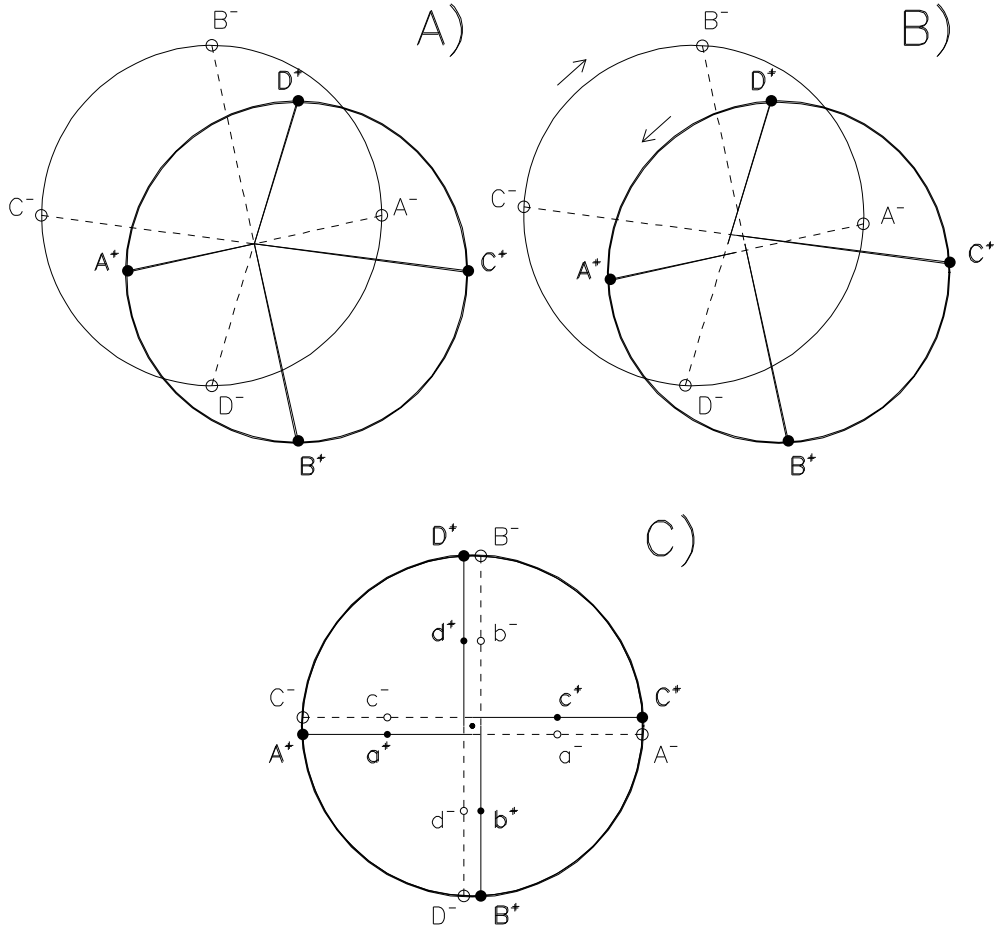


Figure 14: A) Perspective view of an ideal VD, perfectly aligned, with 4 particular muon pair tracks traversing Outer layer at $Z = -10$ cm and $Z = +10$ cm. B) Distorsion of Fig. A when simulating an overall twist induced during the insertion of the VD inside DELPHI. C) $R\phi$ projection of Fig. B where the Closer hits of the 4 muon pair tracks are represented as they are set by the $R\phi$ alignment of the Closer layer modules. The 4 single tracks a^+A^+ , b^+B^+ , ... have impact parameters with a sign opposite to those of the 4 single tracks a^-A^- , b^-B^- ,